Research Article

Mechanical behaviours of hybrid ensete/sisal fiber, reinforced polyethylene composite materials for injection moulding

Bisrat Seifu[1] · Balkeshwar Singh[2] · Moera Gutu J.[2] · Dejene Legesse[3]

Received: 18 November 2019 / Accepted: 2 April 2020 / Published online: 30 April 2020

Abstract
The present research work describes the development and characterization of a new set of natural fiber-based polymer composites consisting hybrid of false banana(Ensete) and sisal fibers as reinforcement and low-density polyethylene (LD-PE) and linear low-density polyethylene (LLD-PE) as polymer matrix and kaolin clay as filler using injection molding technique. This work aims to minimize the cost of raw materials needed for the plastic composite product fabrication process and optimized the composite manufacturing techniques on the injection molding process. In the present work, the effect of hybridization on mechanical properties of Ensete and sisal reinforced polyethylene (ESRF-PE) composite has been evaluated experimentally concerning their mechanical characteristics. The hybrid composites which contains 15% sisal and Ensete fiber with 75% LLD-PE matrixes (Composition, C_3 at T_2) have more tensile, flexural and compression strength than other composites can withstand the tensile strength of 66 MPa and flexural strength of 11.94 MPa and compression strength of 56.5 MPa followed by 20% sisal and Ensete fiber with 70% of the same matrices (composition C_2 of T_1 and $T_{2)}$ which holds 65 and 9.95 MPa respectively, which is 56.58%, 163.90%, and 69.43% higher than that of the non-reinforced PE respectively. It has been observed that the tensile strength of LD-PE-ESRF composite materials have an increase of about 9.92%, 39.60% and 25.62% concerning 15/75 (C_1), 20/70 (C_2), and 25/65 (C_3) composition of fiber to matrix ratio. The water absorption in hybrid composites has been negligible. Because in 24 h, maximum and minimum water uptake has gain 0.1 and 0.6% respectively. To conclude, the highest rate of water uptake of natural fiber composites was 16.31%, which was obtained at 225 °C processing temperature and 25% fiber loading in 240 h. The results demonstrate that hybridization plays an important role in improving the mechanical properties of composites. Experiments are carried by keeping the volume ratio of Ensete and sisal (E:S) 2:3, 3:2 and 1:1, while the Shakiso kaolin was kept constant at 10%. The processing temperatures for injection molding(T_1, T_2, and T_3) were 180, 200, 250 and 220, 250, 285 °C for LD-PE and LLD-PE respectively (the machine has five heating zone/areas), the last corresponding to the injection nozzle. The pressure, injection speed and screw position for LD-PE/LLD-PE were given as – 50/76 kg/cm^2, 48/50% and 55.5/62 mm, respectively. The water absorption result, tensile, compression and flexural properties of these composites are markedly improved as compare to un-hybrid composites. Finally, the surface microstructure test has been done using an optical microscope to study a qualitative evaluation of the interfacial properties of Ensete and sisal reinforced fibers with polyethylene composite.

Keywords Hybrid composites · Polyethylene · Mechanical properties · Injection molding · Moisture absorptions · Diffusivity · Optical microscope

✉ Balkeshwar Singh, balkeshwar71@rediffmail.com; Bisrat Seifu, bisratseifu8@gmail.com; Moera Gutu J., jirata2010moti@gmail.com; Dejene Legesse, degenehareg@gmail.com | [1]Department of Metal Manufacturing, Adama Polytechnic College, Adama, Ethiopia. [2]Department of Mechanical Design and Manufacturing Engineering, Adama Science and Technology University, Adama, Ethiopia. [3]Department of Metal Manufacturing, Metal Industry Development Institute, Addis Ababa, Ethiopia.

SN Applied Sciences (2020) 2:989 | https://doi.org/10.1007/s42452-020-2679-2

1 Introduction

Now a day's the number of plastic manufacturing companies in developing country is steadily growing. They are using various kinds of products made by plastics. So, plastic has become part of lives [1]. But much more important things than these number is their disposal impact on environmental concern and lack in the application of modern technologies, knowledge and scientific tools for these processes.

One of the methods /technologies used to reduce the amount of synthetic plastics is to add natural material into the plastic. This required a detail evaluation process for the performance of the composite product in terms of finding alternative materials that can be used in various engineering applications [2]. Also, there is enormous potential for the production of natural fiber followed by their suitable agro-ecological zones and availability of water in the country. But, few research papers are available on the fabrication of polyethylene-based fiber-reinforced composite materials consisting of hybrid sisal and ensete reinforced-fiber composite [3]. Natural fibers are not only strong and lightweight but also relatively very cheap and low density [4]. **F**or this purpose, attempting to develop a viable substitute for plastics and finding input raw material sources and methods for the production of composite materials is paramount important additions to the existing knowledge and literature in the composite manufacturing area.

Combining the useful properties of two different materials, cheaper manufacturing cost, versatility, etc., makes them useful in various fields of engineering, high-performance applications such as leisure and sporting goods, shipping industries, aerospace industries, etc. [5]. Hence, with this background, it is concluded that the composites stand the most wanted technology in the fast-growing current trend [6]. From the above results, the hybrid composite is found to the best option for all general application The application of these fibers as a substitute for synthetic fibers because they have relatively high strength, stiffness, and low density and also they are renewable energy sources, environmentally friendly, biodegradable, cheaper, have less harmful to humans, machinery and the environment, thus being realistic alternatives to glass fiber [7].

Hybrid composites are the systems where one type of reinforcing or filler material is incorporated or added in a mixture of dissimilar or different matrices (blends), or two or more reinforcing or filling materials are present in a single matrix or, also, both approaches are combined [8]. The hybridization of two fibers in a composite always gives better behavior than single fibered composites [9]. Mechanical strengths of composites reinforced with different natural fibers have been investigated by several researchers. The effect of various parameters like alkali treatment, fiber loading and hybridization effect of natural fiber-reinforced composites have been studied [9–11].

Research work on Ensete fiber-reinforced composites reported that a useful composite with good properties could be successfully developed using Ensete fiber as a reinforcing agent. The results also indicate that fiber orientation, matrix type, fiber thickness are the significant factors in determining the mechanical properties of the composite using Ensete as reinforcing material [12]. It is also observed that Ensete has better mechanical properties such as tensile strength, flexural strength, and compressive strength compared to banana fiber [12, 13].

Natural fiber composites (NFC) manufacturing techniques include press molding, extrusion, injection molding, compression molding and resin transfer molding [14]. Extrusion is a widely practiced processing method and the majority of the current bio-composite materials based on thermoplastic polymers are processed by this method [15].

Injection molding is a process of forming a product by forcing molten plastic material under pressure into a mold where it is cooled, solidify, and subsequently released by opening the two halves of mold [16]. Injection molding is a primary processing method used in a variety of applications in both commercial and research fields which is well suited for mass production of goods because the raw material is converted to finished part usually in one operation [17, 18]. There are three main stages in the injection molding cycle; stage 1, injection, followed by stage 2, holding pressure and plasticizing, and finally, stage 3, ejection of the molded part. When stage 3 is completed the mold closes again and the cycle starts over again [19].

The results of this present study showed that a useful composite with good properties could be successfully developed using a hybrid of sisal and Ensete fibers as a reinforcing agent. The results also indicate that; fiber loading, matrix type, composite fabrication techniques and processing temperatures of injection molding machine are the significant factors in determining the mechanical properties of the composite using ensete and sisal as reinforcing materials.

2 Materials and methods

2.1 Materials

2.1.1 Reinforcement material

For the present research work, Ethiopian fibers of the plant *Ensete ventricosum* (false banana) and sisal fibre are employed as reinforcement materials for the composite fabrication process in the experiment as shown in Fig. 1a and c respectively. The sisal fibers used for this study were collected from Wonji, Oromia region, Ethiopia. Here the fibers were extracted manually from the plant leaves shown in Fig. 1d, while false banana fiber was bought from the local market as shown in Fig. 1b. The experiment used fibers from the plants grown in plantations in Ethiopia were preferred mostly, since they are eco-friendly and also available at less cost. Both fibers were then washed cleanly in water to eliminate dirt and other foreign particles and then kept in sunlight up to 12 h to remove water from fibers.

These fibers were cut with scissor randomly an approximate length of about 10–15 mm as shown in Fig. 1e and then soaked separately with 4 wt% sodium hydroxide (NaOH) solution into chopped fibers for 24hrs to ensure good and uniform penetration of the solution shown in Fig. 1f. After that, the treated fibers were subsequently kept in sunlight for 12 hr, then they become dry and strong fibers and this makes to grind them easily shown in Fig. 1g. Finally, the dried fibers were ground in SR 200 Gusseisen Mill machine and its power, voltage, and frequency of the machine are given by 1.1 kw, 230 v and 50 Hz respectively at "Forest Products Utilization Research Center", Addis Ababa. Saris, as shown in Fig. 1h and sieved with a sieve size of 0.15 and 0.3 mm shown in Fig. 1i and the sieved fibers are shown in Fig. 1j below. The Shakiso clay that obtained from "Awash Melkasa Aluminum Sulphate and Sulphuric Acid Share Company" was also sieved with the same sieve size.

2.1.2 Matrix material

In this study, Polyethylene was used as the matrix, supplied by Metal Industry Development Institute (Addis Ababa, Ethiopia). The LLD/LD Polyethylene's used were 4025 TASNEE from National Petrochemical industries, Saudi Arabia and Lotrène FD0474 from Qatar Petrochemical Company,

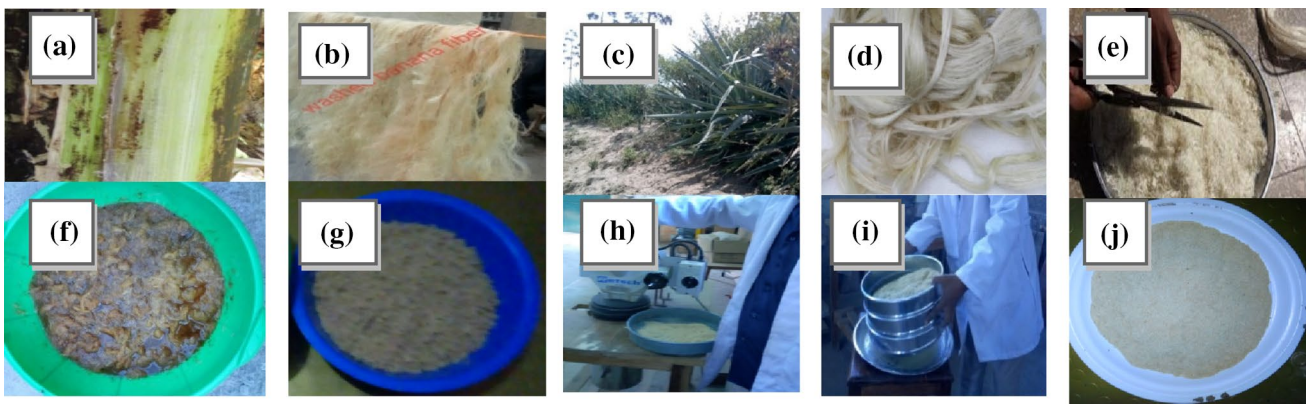

Fig. 1 Ensete and sisal plant fiber: **a** stem of ensete, **b** washed ensete, **c** sisal plant, **d** extracted sisal fiber, **e** chopped fiber, **f** soaked fiber, **g** sun-dried fiber, **h** fiber grinding, **i** fiber during sieving, **j** fiber after sieving

Table 1 Characteristics of the polyethylene used in this study

Characteristics	LLD-PE			LD-PE		
	Test methods	Value	Unit	Test methods	Value	Unit
Melt Flow Index	ISO 1133	4.0	g/10 min	ASTM D-1238	4.0	g/10 min
Melting point	ISO 3146	111	°C	ASTM E-794	108	°C
Density	ISO 1183	0.925	g/cm^3	ASTM D-1505	0.923	g/cm^3
Tensile strength at yield	ISO 527-1,-2	11	MPa	ASTM D-882	11/11	MPa
Elongation at yield	ISO 527-1,-3	300/600	%	ASTM D-882	335/610	%
Tensile modulus	ISO 527-1,-2	260	MPa	ASTM D-882	23/20	MPa
Impact strength, F 50	ASTM D 1709	100	G	ASTM D-1709	90	G

Qatar respectively. Characteristics of polyethylene which given by the manufacturer as shown in Table 1.

2.2 Methods

2.2.1 Composite mixing method

The density of the Ensete/sisal particulate and Shakiso kaolin clay (in the powdery state) was determined using the reference with a known standard true density of composite materials. Their constitutes were 2.6, 0.668 and 1.33 g/cm^3 for kaolin clay, Ensete and sisal fiber particulates respectively [18]. The Shakiso kaolin was kept constant. Keeping the volume ratio of Ensete and sisal (*E*:*S*) 2:3, 3:2 and 1:1, the Ensete and sisal particulates composition of mixed hybrid composites were prepared at different fiber loading of required grain sizes are weighed and kept in a different bowl, 0.15–0.25 V_f as shown in (Fig. 1). LD-PE/LLD-PE and hybrid particles of Ensete/sisal were varied accordingly from 75%, 70%, 65% and 15%, 20%, 25% respectively. The Shakiso kaolin was kept constant at 10%. The composition of the constituents by weight is given in Table 2 in detail.

2.2.2 Mass of composite calculation methods

The mass (*m*) was determined with the aid of a digital weighing balance machine and packed in a different composition. The density of the composites (ρ_c) was determined by measuring the mass and volume (*v*) of the sample composite according to (ASTM D7929, 2013) standard. The volume of each composite sample was found using Archimedes's principle.

The density of each sample was determined as follows. Thus density is given as:

$$\rho = \frac{m}{v}\ (\mathrm{g/cm^3}) \tag{1}$$

The volume of the composite was calculated by multiplying the length, width and depth of the mold prepared for molding the composite material by Eq. (2) and the density of the composite was calculated by a method which enable the rule of law of mixture to be applied and was obtained first by adding the volume fraction of polyethylene (both LD-PE and LLD-PE) and hybrid of Ensete and sisal fiber for each fiber/matrix ratio. The density of the composite was obtained by Eq. (3). After getting the density of the composite then the mass of each composite (fiber, filler, and matrix) was obtained according to Archimedes's principle by multiplied the volume with a density of the composite by Eq. (4). Then finally the density of sisal and Ensete fibers, kaolin clay, LLD-PE, and LD-PE matrix was taken as 1.33, 0.668, 2.6, 0.925 and 0.923 g/cm^3 respectively.

2.2.3 Weight composition

The composites have a three-constituent composition, consisting of LD-PE and LLD-PE as a matrix, Ensete and sisal as reinforcement and Shakiso kaolin clay as a corresponding filler. The composite mixtures were prepared depending on the weight fraction, which was determined based on the volume of the composite material. Total raw materials used for composite mixtures were kaolin clay (700 g), low-density polyethylene (LD-PE, 6500 g), false banana fiber particulate (1000 g), sisal fiber particulate (9000 g) and linear low-density polyethylene (LLD-PE, 6500 g). Based on the literature review, the mixing proportion of Ensete/sisal, LDPE and kaolin are obtained according to weight mixture proportion [20]. The particulate (fiber) was varied from 15 to 25%, LD-PE/LLD-PE where varied accordingly from 65 to 75% and the Shakiso clay was used at 10% only. The composition of the constituents in percentage is given in Table 3.

On the estimation of required percentage weight fraction of these fibers and matrixes were found. Based on the

Table 2 Method of calculating the mass of composite materials

Volume of the die (V_c) = Length × Width × Depth (2)	
Volume of the die (V_c) = 162.35 × 218 × 3 = 106,176.9 mm^3 = 106.177cm^3	
Density of the fibers/matrix in g/cm^3 (density = mass/volume (or) volume = mass/density)	
$V_c = V_{matrix} + V_{fiber} + V_{filler}$	
$M_c/\rho_c = M_{matrix}/\rho_{matrix} + M_{fiber}/\rho_{fiber} + M_{filler}/\rho_{filler}$ (3)	
For LLD-PE	For LD-PE
$1/\rho_c = (0.65/0.925) + (0.25/1.998) + (0.1/2.6)$	$1/\rho_c = (0.65/0.923) + (0.25/1.998) + (0.1/2.6)$
$1/\rho_c = 0.7027 + 0.1251 + 0.0338 = 0.8616$ cm^3/g	$1/\rho_c = 0.7042 + 0.1251 + 0.0338 = 0.8631$ cm^3/g
$\rho_c = 1.1606$ g/cm^3	$\rho_c = 1.1586$ g/cm^3
$\rho_c = 1.1606$ g/cm^3/1.1586 g/cm^3 (For 25% of hybrid of Sisal/Ensete fiber-reinforced LLD-PE/LD-PE Composite materials).we use the same calculation for 20% and 15% of hybrid Sisal/Ensete fiber-reinforced LLD-PE/LD-PE composite materials	
$M_c = \rho_c \times V_c$ (4)	
$M_c = 1.1606 \times 106.177 = 123.23$ g	$M_c = 1.1586 \times 106.177 = 123.02$ g

literature review, the mixing proportion of Ensete/sisal, LDPE and kaolin are obtained according to weight mixture proportion [20]. The composition of hybrid Ensete/sisal fiber and LD-PE/LLD-PE was varied. The particulate (fiber) was varied from 15 to 25%, LD-PE/LLD-PE were varied accordingly from 65 to 75% and the Shakiso clay was used at 10% only. The total composite materials comprising were obtained 15.6 kg. The working parameters were used 80 rpm for 2 min on the mixing machine as shown in Fig. 2a and b shows composition constitute by weight percent.

2.2.4 Experimental procedures

The experimental works required for this study were carried out in the Institute of Metal Industry Development Center. The hybrid composite of ensete/ sisal fibre was fabricated by the injecting molding techniques using injecting molding machine, SHIN HYDRAULICS CO.LTD **220** was used to produce several sets of telephone terminal box closure pieces out of two different natural fibers and two composite materials of different properties, sisal/false banana and LD-PE/LLD-PE respectively.

2.3 Injection mould component description

The mold clamping size used for fabrication of composite is made from mild steel 308 × 386 mm in size. The cavity and core of the mold, which means the size of the composite component is given by 218 × 193 mm in size. The mold used for the fabrication of the composite is presented in Fig. 3.

2.3.1 Process characteristics

The mixing technique of fibers with a polyethylene matrix used for this study was a melt mixing forming technique with injection molding. The LD/LLD-PE plastic composite materials, usually in the form of granules, are fed from a hopper on to the screw. It is then conveyed along the barrel where it is heated by conduction from the barrel heaters and shear due to its movement along the screw flights. The depth of the screw channel is reduced along the length of the screw to compact the material. At the end of the extruder, the melt passes through a die by the runner to mold cavity where it cools and hardens to the configuration of the cavity and finally produced the desired shape of terminal box closure components as shown in Fig. 3c by using injection machine in Fig. 4. Injection processing temperature for composite materials is shown in Table 4.

Table 3 Mass of composite specimen

Designation	Composition									No of samples
	Weight in (%)					Mass (g)			Total in (g)	
	Fibers		Matrixes	Fillers		Fibers	Matrixes	Fillers		
	E (wt %)	*S* (wt %)	*E* + *S* (wt %)	LLD-PE/LD-PE (wt%)	Kaolin (wt%)	*E*/*S* (g)	LLD-PE/LD-PE (g)	Kaolin (g)		
C_3 (25)	10	15	25	65	10	30.81/30.75	80.1/79.9	12.32/12.30	123.2/123.0	1
C_2 (20)	10	10	20	70	10	23.84/23.78	83.4/83.2	11.92/11.89	119.2/118.9	1
C_1 (15)	9	6	15	75	10	17.32/17.28	86.6/86.4	11.55/11.52	115.5/115.2	1
LD/LLD	-	-	-	100	0	0	98.7/98.5	0	98.76/98.54	1

2.3.2 Specimen sampling procedure

The entire composite specimen used for testing were cut from the layout parts of terminal box closure composite laminates. Circular and portable jig saw machines are used for cutting straight and curved lines of the specimen respectively, as shown in Fig. 4. The specimens were cut from the centers of the composite laminates, to minimize the edge defects. Dog bone-shaped specimens were used for tensile and while flat specimens were used for flexural and other tests as mentioned in Sect. 2.4. The prepared specimen is shaped into the required dimension using a circular saw machine as shown in Fig. 5b and the edges

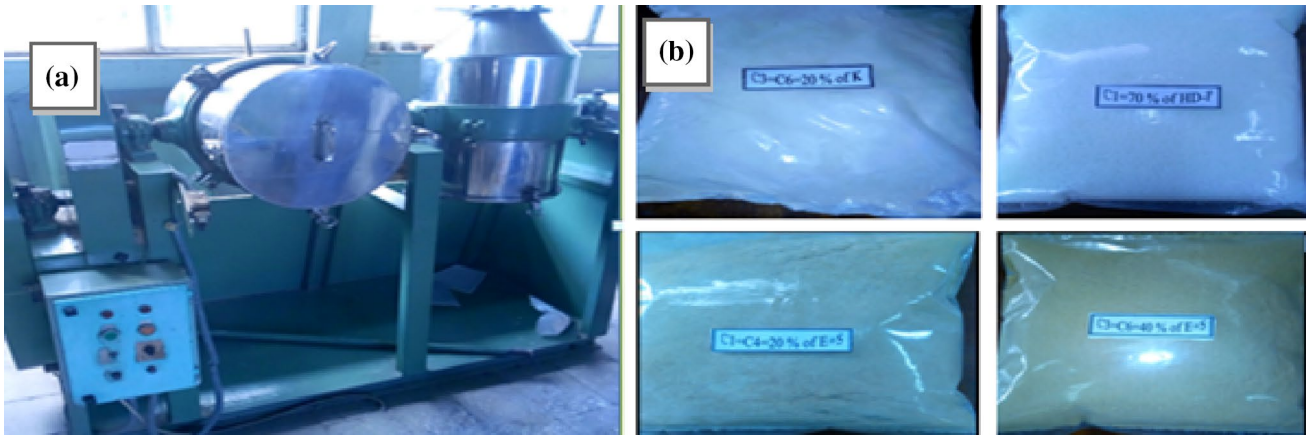

Fig. 2 **a** Composition mixing machines, **b** Composition constitutes by weight in (%)

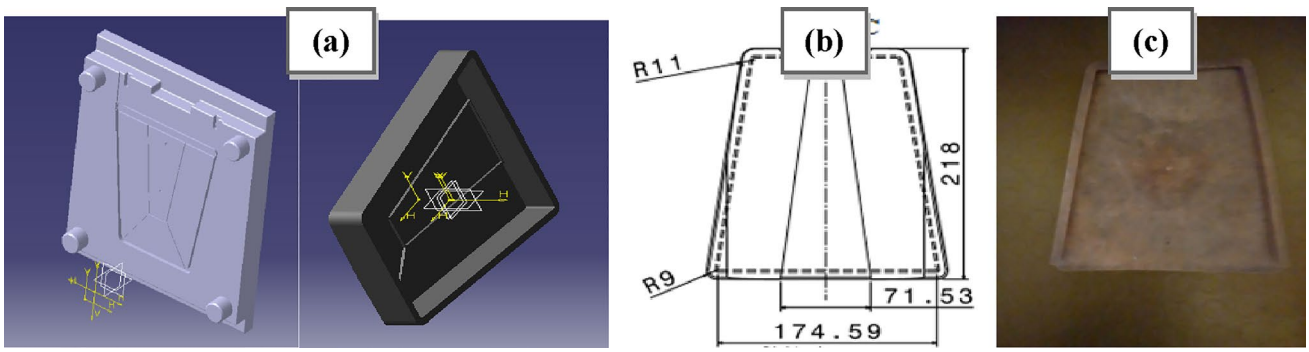

Fig. 3 The mold used for fabrication of the composite: **a** box closure specimen mold cores and 3D view. **b** Mold size for box closure specimen, **c** composite product

Fig. 4 Injection molding process

are polished using the sandpaper after making a sample profile on the vertical rotating machine as shown in Fig. 5c. The dimensions, gauge length, and crosshead speeds are chosen according to the ASTM standard.

2.4 Determination of mechanical properties of composite materials

2.4.1 Tensile strength test (ASTM D-3039)

The ensete and sisal hybrid fiber reinforced LD/LLD-PE composites were prepared with the fabricated samples and tested in the Universal tensile testing machine (UTM) under room temperature with all volume fractions. The most important mechanical property of composite material is its stress–strain curve which is obtained by stretching a sample in a tensile testing machine and measuring the sample`s extension and the load required to reach this extension as shown in Fig. 6b. The elongation strain ε is calculated using the following equation $\varepsilon = \Delta L/L_0$, Where $L - L_0 = \Delta L$ is the change in gauge length, L_0 is the initial and L the final lengths, respectively. The force measurement is used to calculate the stress (σ), given by equation $\sigma = F/A$ Where F is the tensile force and A is the initial cross-section of the sample.

The apparent stress–strain curve can be plotted. Tensile properties can be deduced from that plot, such as Young's modulus, ultimate tensile strength, and

Table 4 Injection process temperature for composite materials

Composite materials	Process temperatures	Nozzle Temp (°C)	Cylinder.1 (°C)	Cylinder.2 (°C)	Cylinder.3 (°C)	Cylinder.4 (°C)
LLD-PE	T_1	175	199	195	205	220
	T_2	220	225	230	230	250
	T_3	250	260	275	275	285
LD-PE	T_1	140	160	170	170	180
	T_2	180	185	190	190	200
	T_3	200	210	220	220	250

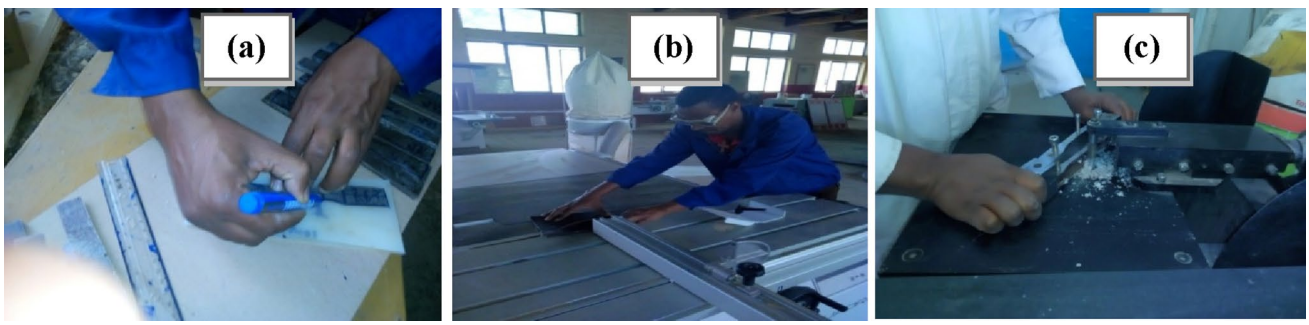

Fig. 5 Tensile test specimen preparation process: **a** tracing a sample, **b** cutting with a circular saw, **c** making a sample profile

Fig. 6 **a** Specimen samples after cutting, **b** Specimens under tensile strength test

elongation at failure. Tensile testing of the composites was carried out according to the ASTM D-3039 standard using the Shanghai Bairoeuniversal testing machine at Addis Ababa Technical and Vocational Training Institute. The dog bone-shaped specimens as shown in Fig. 6a were clamped and pulled apart using a 5-kN load cell. The overall length of the specimen was 200 mm which includes a 120 mm parallel-sided portion. The parallel-sided portion's width was 12.7 mm and the width at the ends was 25 mm. The gauge length was 90 mm and the rate of loading was 10 mm/min.

The primary objective of this test was to evaluate the hybrid tensile properties of Ensete and sisal fiber composites. For each sample, 9 specimens were tested in each machine and cross-machine-direction each specimen was 25 by 200 mm during the test specimens were placed in the grips of UTM and axial load is applied through both the ends of the specimen. There are three different components of samples are prepared according to the ASTM standards and the experiments are repeated several times and the average values are used for discussion.

2.4.2 Flexural strength test (ASTM D790-2010)

Flexural strength, σ_f, was obtained from the critical load, F, with the help of the relation, $\sigma_f = 3FL/2bd^2$, where L was the distance between the supports, b and d are width and thickness of specimen respectively. The flat specimens dimension for the flexural test was 165 mm length, 25 mm width and 6 mm thickness and placed with support at two ends and the force was applied in the middle as shown in Fig. 7.

2.4.3 Compressive strength test (ASTM D-3410)

The Compression strength of the ensete and sisal reinforced (ESR) fibers with PE was determined by a manually controlled compression testing machine found at Addis Abeba construction biro as shown in Fig. 8b Compressive test specimens were prepared as random orientation three types of ESR to/polyethylene with the fiber/matrix ratio of (15/75, 20/70 and 25/65) were used for both LD-PE and LLD-PE composite specimen for each ratio as shown in Fig. 8a.

2.4.4 Water absorption behavior of composite

The water absorption characteristics of sisal/ensete hybrid fibre reinforced polyethylene composite were studied by immersion in distilled water at room temperature for 24, 48, 72, 96, 120, 144, 168, 192, and 216 and 240 h as shown in Fig. 9b. Moisture absorption and volume swelling tests were conducted under ASTM D570.

Ten specimens for different fiber composition (15%, 20%, and 25%)and temperature range were cut with dimensions of 25 × 25 × 3 mm (length × width × thickness) and the samples was dried for 8 h at 80 °C before immersing in water and allowed to cool at room temperature (Fig. 9a) then the weight of the sample was taken before and after immersed to distill water environment using a balance electro mass testing machine having a precession of 0.0001 g accurately as shown in Fig. 10b. After exposing for 24 h. Samples were taken out of the water after the appropriate period and wiped with a clean dry cloth to remove surface water. The specimens were reweighed to

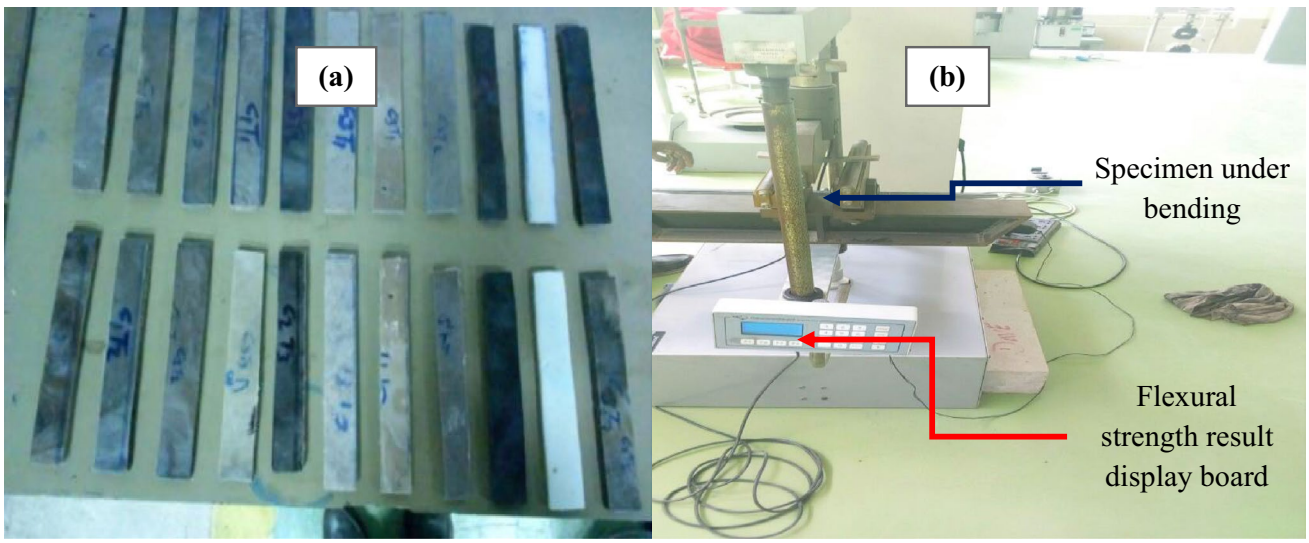

Fig. 7 **a** Specimen Sample after cutting, **b** Specimen failure under flexural loading

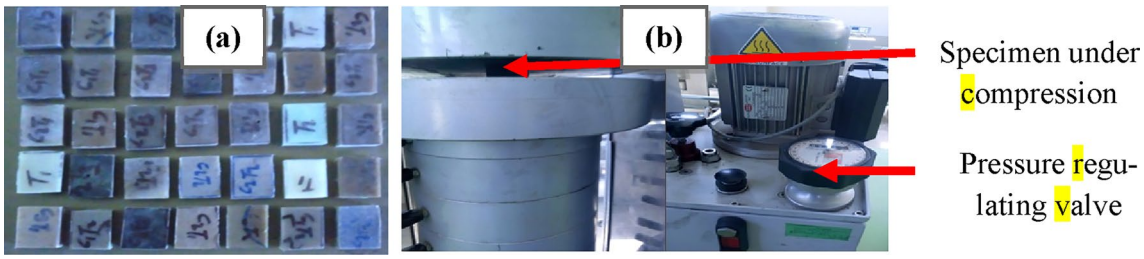

Fig. 8 **a** Specimen Sample after cutting, **b** Specimen failure under compression loading

Fig. 9 **a** prepared samples for H_2O moisture test, **b** Specimen at water absorption test

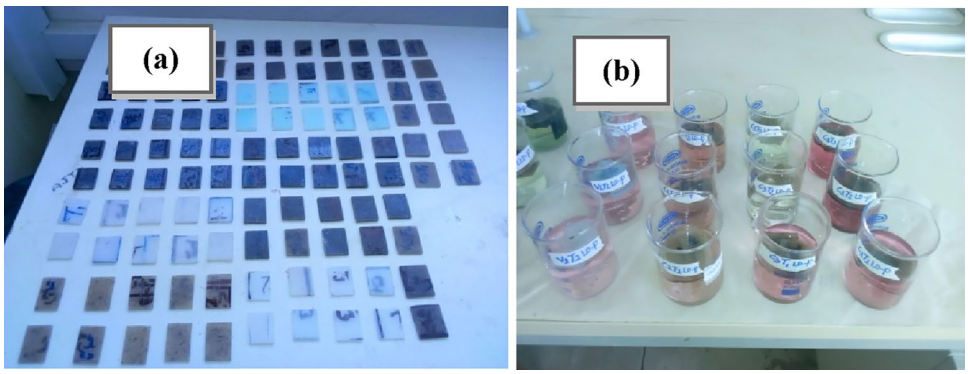

Fig. 10 **a** Measuring Specimen in digital caliper, **b** Specimen at balance weight

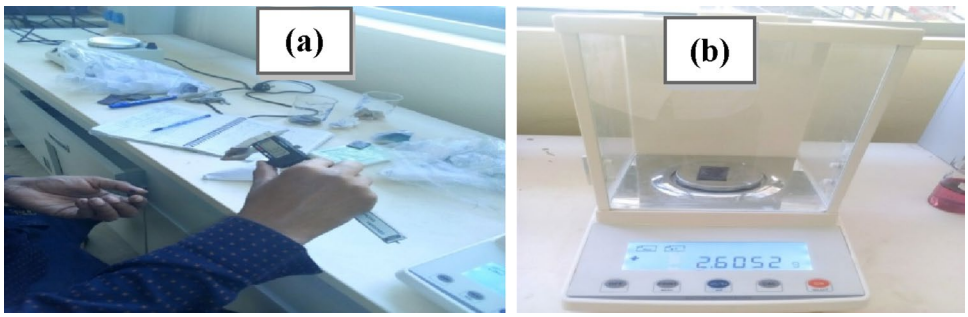

the nearest 0.0001 g within 1 min. of removing them from the environment chamber. The specimens were weighed regularly from 24–240 h with a gap of 24 h of exposure. The percentage weight gain of the samples was measured at different time intervals by using the following equation:

$$\text{Moisture absorption}\% = \frac{W2 - W1}{W1} \times 100\% \quad (5)$$

where, W_1 = Initial weight of composite, W_2 = Final weight of composite after immersion in water.

Apparatus Digital Caliper used to measure the length, width, and thickness of samples and weighing scale capable of determining mass to 0.0001 g. *Pre-test procedure* a table was prepared for the recording of the data and the specimen name and size.

The specimen was measured on each side with digital calipers (since the specimen was not uniform multiple points were measured and the average value was obtained) and the measurements recorded to the nearest mm as shown in Fig. 10a.

The test method was recorded. The volume swelling (VS) of the sample was determined by using the following equation:

$$V_s(t) = \frac{V_2 - V_1}{V_2} \times 100 \quad (6)$$

where 'V_2' and 'V_1' are the composite's volumes after and before immersion in water respectively.

Change in volume of composite was calculated by: Volume = (length × width × thickness) = 33.89 × 26.35 × 2.96 = 2643.28 mm^3 = V_1, 33.94 × 26.37 × 2.96 = 2649.19 mm^3 = V_2.

$V_{C_1T_1}(24) = \frac{2649.19-2643.28}{2649.19} \times 100 = \frac{5.91}{2649.19} \times 100 =$ **0.223** percent of volume in change for (C_1T_1hybrid of Sisal/Ensete fiber LD-PE Composite materials). We use the same calculation for T_2 and T_3 of each fiber-reinforced LLD-PE/LD-PE composite materials at different fiber loading and time variation.

2.4.5 Method of microstructure tests sampling

The first step of sample preparation is cutting the composite materials having a length of 20 × 20mm^2 of three different samples of 25, 20 and 15 wt% of composite by abrasive cutter. When doing this water is a bulb on around the blade to save the blade and keeps the surface of the specimen from destroying. This is interesting that water recycled to clean the abrasive cutter using a Pentium air compressor. The preparation of the sample surface requires great care to have a good image quality suitable for characterizing the fibre microstructure. The sample is firstly polished by abrasives, starting with coarse ones and finishing with fine ones, and secondly polished by diamond paste. At least a difference in depth of 100 µm was needed between two successive layers to avoid scratches and to get a polished surface possible for analyzing. The sample was analyzed with optical microscopy in reflection mode, and 5 mm × 5 mm cartographies were recorded by assembling "elementary" images.

3 Results and discussions

3.1 Tensile properties

For tensile strength evaluation, there were 9 specimen groups for each matrix type (LD-PE/LLD-PE) at (three different temperature ranges T_1, T_2, and T_3) and fiber/matrix ratio (15/75, 20/70 and 25/65) total of 36 specimens were prepared. The influence of fiber loading and processing temperature change on tensile properties of composite material is shown in Tables 5, 6, and 7. It has been observed that the tensile strength of composites increases with an increase in fiber loading and decreases in increasing processing temperature.

3.1.1 Tensile modulus of elasticity graph

The modulus of elasticity was calculated using Eq. (7).

$$E = \frac{\text{Stress}}{\text{Strain}} = \frac{F}{e} \times \frac{l}{A} \tag{7}$$

where F = force, e = extension, l = original length and A = cross-sectional area.

In the case of LD-PE, as shown in Fig. 11, It has been observed modules of elasticity of C_1 fiber composition is higher than C_3 fiber composition. But in the case of LLD-PE, as shown in Fig. 12, modulus of elasticity of C_3 fiber composition is higher than C_1 fiber composition. In LD-PE composite materials, the tensile modulus of elasticity increases when injection temperature increases as shown in Fig. 13, while in the case of LLD-PE composite materials, the tensile modules of elasticity decreases as injection temperature increases as shown in Fig. 14.

Where, C_1 = 15/65, C_2 = 20/70 and C_3 = 25/75% of fiber to matrix ratio respectively and the rest 10% is the kaolin clay, while T_1 = 180/220, T_2 = 200/250 and T_3 = 220/285 are injection temperatures for the LD-PE and LLD-PE respectively. Fiber/matrix ratio did affect the tensile strength of

Table 5 Results for tensile specimen C_1

Designation	For LD-PE composite materials		For LLD-PE composite materials	
	Maximum force in (KN)	Tensile strength in (MPa)	Maximum force in (KN)	Tensile strength in (MPa)
C_1T_1	1.4	37	2.3	61
C_1T_2	1.6	41	2.3	60
C_1T_3	1.5	40	1.5	40

Table 6 Results for tensile specimen C_2

Designation	For LD-PE composite materials		For LLD-PE composite materials	
	Maximum force in (KN)	Tensile strength in (MPa)	Maximum force in (KN)	Tensile strength in (MPa)
C_2T_1	1.4	38	2.5	65
C_2T_2	1.5	38	2.1	55
C_2T_3	1.2	31	1.2	20

Table 7 Results for tensile specimen C_3

Designation	For LD-PE composite materials		For LLD-PE composite materials	
	Maximum force in (KN)	Tensile strength in (MPa)	Maximum force in (KN)	Tensile strength in (MPa)
C_3T_1	0.2	5	2.4	62
C_3T_2	1.1	28	2.5	66
C_3T_3	1.1	28	0.2	5

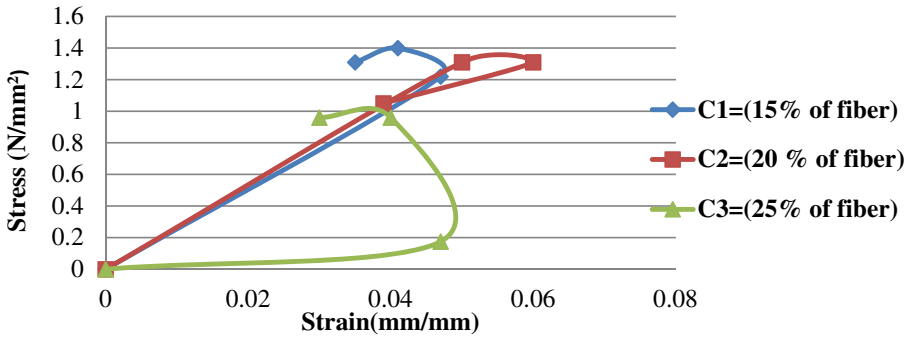

Fig. 11 Stress–Strain Comparison graph for LD-PE composite materials

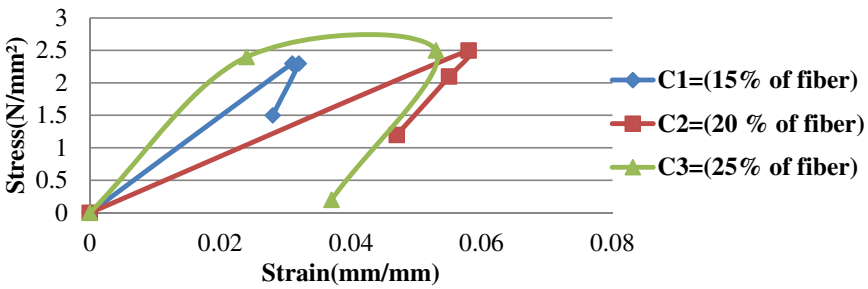

Fig. 12 Stress–strain comparison graph for LLD-PE composite materials

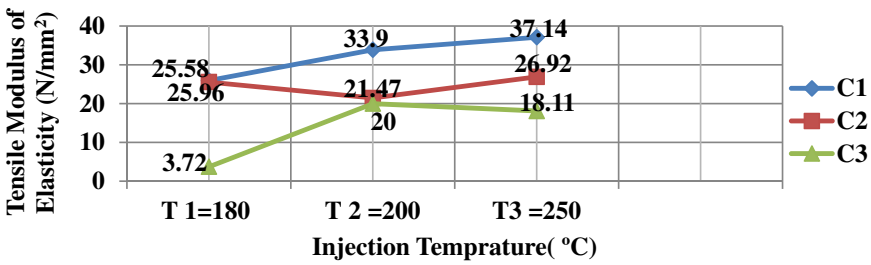

Fig. 13 Tensile modulus vs injection temperature for LD-PE composite materials

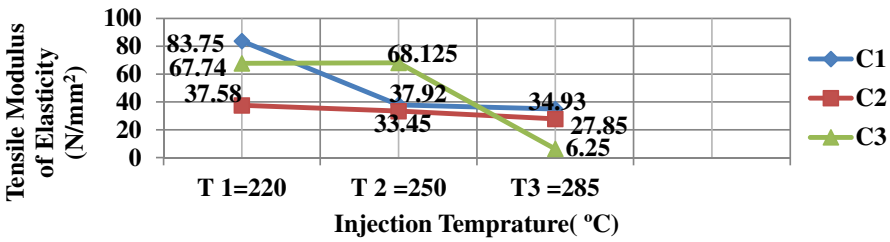

Fig. 14 Tensile modulus vs injection temperature for LLD-PE composite materials

the sisal with ensete fiber-reinforced polyethylene composite materials, comparing the maximum strength levels for the LD-PE and LLD-PE batch of ESR composite, for example, the tensile strength of LD-PE-ESRF composite shows an increase of about 9.92%, 39.60% and 25.62% between 15/75, 20/70, and 25/65 respectively according to this results, the fiber—matrix ratio and variation of injection temperature have a significant effect on tensile strength with increasing and decreasing of fiber content and temperature range in the composite making process.

3.2 Bending properties

The influence of fiber loading and temperature on the flexural strength of fabricated composites is shown in Tables 8, 9, and 10. It shows that when fiber loading increases, then the flexural strength also increases in LD-PE from 5.97 to

Table 8 Results for flexural specimen C_1 (15%)

Designation	LD-PE		LLD-PE	
	Load in (N)	Flexural Strength in (N/mm^2)	Load in (N)	Flexural Strength in (N/mm^2)
C_1T_1	10	1.99	30	5.97
C_1T_2	40	7.96	50	9.95
C_1T_3	20	3.98	30	5.97

Table 9 Results for flexural specimen C_2 (20%)

Designation	LD-PE		LLD-PE	
	Load in (N)	Flexural strength in (N/mm^2)	Load in (N)	Flexural strength in (N/mm^2)
C_2T_1	20	3.98	40	7.96
C_2T_2	30	5.97	50	9.95
C_2T_3	20	3.98	40	7.96

Table 10 Results for flexural specimen C_3 (25%)

Designation	LD-PE		LLD-PE	
	Load in (N)	Flexural strength in (N/mm^2)	Load in (N)	Flexural strength in (N/mm^2)
C_3T_1	20	3.98	30	5.97
C_3T_2	30	5.97	60	11.94
C_3T_3	20	3.98	30	5.97

7.96 MPa but decrease in LLD-PE from 11.94 to 9.95 MPa of fabricated composite materials. The maximum flexural strength is observed for each fiber loading of temperature T_2 (225 °C/250 °C) for LD-PE and LLD-PE composite materials respectively**.**

3.2.1 Flexural modulus

The Flexural modulus, E, was obtained from the critical load, F_{max}, with the help of the relation, $E = 4\boldsymbol{F}_{max} \times L^3/3\boldsymbol{D}\boldsymbol{\pi}d^4$, where L was the distance between the support loads in (mm), D and d are deflections in (mm) at F_{max}, and diameter of specimens in (mm) respectively. The results of flexural modules of elasticity of composite materials are given in Table 11.

3.3 Compression properties

It was found that the compressive strength kept increasing with the increase in fibre content from 15% fibre content to 25% fibre content. At 15% fibre content, the compressive strength decreased because the interfacial adhesion between fibers and PE was not good therefore reducing the compression force applied to it. It was also seen that composite with 25% fibre has the best compressive strength than other fiber content composition. It was observed that the rate of water absorption in the composite increases as the percentages of fibers decrease and increasing injection molding temperature respectively as shown in Tables 13 and 14 and also the composite increases with immersion time although the rate of absorption decrease with increased time after a week. Tables 12, 13 and 14 shows the result of compressive strength. V_1, V_2 and V_3 indicate the virgin materials at injection temperature T_1, T_2, and T_3 respectively.

3.4 Moisture absorptions

Tables 15, 16, 17, 18, 19 and 20 shows the result of water absorption test of LD-PE and LLD-PE reinforced composite after expose to a different environment for a period of 240 h The water absorption in hybrid composites was negligible in 24 h, maximum and minimum water uptake was shown by ensete and sisal hybrid fiber (ESHF) LD

Table 11 Results for flexural modulus of composite materials(N/mm^2)

Composition	LD-PE				LLD-PE			
	Injec. temp (°C)	F_{max}	D (mm)	E (N/mm^2)	Injec. temp (°C)	F_{max}	D (mm)	E (N/mm^2)
C_1	180	10	0.01	4880.7	220	30	0.05	286,583.9
	200	40	0.07	2788.9	250	50	0.09	26,536.5
	250	20	0.03	3253.8	285	30	0.05	286,583.9
C_2	180	20	0.03	31,842.6	220	40	0.07	27,293.7
	200	30	0.05	286,583.9	250	50	0.09	26,535.5
	250	20	0.03	31,842.6	285	40	0.07	27,293.7
C_3	180	20	0.03	31,842.6	220	50	0.09	26,535.5
	200	30	0.05	28,658.3	250	60	0.11	26,053.1
	250	20	0.03	31,842.6	285	30	0.05	286,583.9

Table 12 Results for compression specimen C1 (15%)

Designation	LD-PE		LLD-PE	
	Peak value in (kN)	Specific strength in (N/mm^2)	Peak value in (kN)	Specific strength in (N/mm^2)
C_1T_1	42.7	19.31	20.0	9.04
C_1T_2	124.9	56.15	24.2	10.95
C_1T_3	45.9	20.76	29.0	14.4
V_1T_1	22.54	10.2	23.6	10.67

Table 13 Results for Compression Specimen C_2 (20%)

Designation	LD-PE		LLD-PE	
	Peak value in (kN)	Specific strength in (N/mm^2)	Peak value in (kN)	Specific strength in (N/mm^2)
C_2T_1	20.2	9.14	24.1	10.90
C_2T_2	34.3	51.2	24.4	10.04
C_2T_3	22.2	10.04	24.2	10.95
V_2T_2	22.8	10.31	23.6	10.67

Table 14 Results for compression specimen C3 (25%)

Designation	LD-PE		LLD-PE	
	Peak value in (kN)	Specific strength in (N/mm^2)	Peak value in (kN)	Specific strength in (N/mm^2)
C_3T_1	21.7	9.81	24.5	11.08
C_3T_2	21.9	9.90	26.0	11.76
C_3T_3	25.7	12.78	22.4	10.13
V_3T_3	22.01	10.01	22.5	10.15

and LLD-PE respectively, but after 24 h increases at the rate of 0.01–2.86 and 0.02–16.3% respectively. It was also observed that the composite attains equilibrium after 144 h. However, this is explained by the fact that reinforced natural fiber (RNF) composite material has more tied bonding and less water content compared to non reinforced natural fibers. On the other hand, the injection temperature affects the water absorption values which shows that composites with 25% fibers at higher temperatures have less absorption compared to composites with 20% and 15% fibers with optimum temperature.

This shows that the exceeding temperature in the composite reduces the water absorption of the fibre on terminal box closure parts. The test conducted at ambient

Table 15 Variation of weight gain and change in volume on 15% of fiber content for LD-PE

Time of immers in (h)	Weight of the specimen in (g)						Volume of the specimen in (mm^3)					
	C_1T_1		C_1T_2		C_1T_3		C_1T_1		C_1T_2		C_1T_3	
	Final wt	Wt. gai. in (%)	Final wt	Wt. gai. in (%)	Final wt	Wt. gai. in (%)	Vol. change	Vol.gai in (%)	Vol. change	Vol.gai in (%)	Vol. change	Vol. gai in (%)
0	2.4658	0	2.6326	0	2.8512	0	0	0.00	0	0.00	0	0.00
24	2.4718	0.24	2.6329	0.01	2.8534	0.08	5.91	0.22	32.84	1.11	2.25	0.01
48	2.4757	0.39	2.6362	0.14	2.8565	0.19	35.73	1.33	35.95	1.22	16.15	0.47
72	2.4859	0.81	2.6382	0.21	2.8599	0.30	71.24	2.62	56.62	1.91	25.56	0.74
96	2.4861	0.82	2.6388	0.24	2.8602	0.32	76.71	2.82	72.32	2.43	31.33	0.90
120	2.4866	0.84	2.6404	0.29	2.8645	0.46	83.21	3.05	158.6	5.18	36.86	1.07
144	2.4915	1.03	2.6463	0.52	2.8673	0.56	83.21	4.32	196	6.32	41.14	1.19
168	2.4978	1.28	2.6476	0.57	2.8684	0.60	119.4	4.72	231.5	7.38	66.62	1.91
192	2.4998	1.36	2.6476	0.57	2.8748	0.82	131.0	5.57	253.5	8.02	125.5	3.54
216	2.4999	1.36	2.6477	0.57	2.8749	0.82	155.9	6.14	258.8	8.17	129.1	3.64
240	2.4999	1.36	2.6478	0.57	2.8749	0.82	173.1	6.51	270.9	8.52	139.9	3.93

SN Applied Sciences (2020) 2:989 | https://doi.org/10.1007/s42452-020-2679-2

Table 16 Variation of weight gain and change in volume of 20% of fiber content for LD-PE

Time of immers in (h)	Weight of the specimen in (g)						Volume of the specimen in (mm^3)					
	C_2T_1		C_2T_2		C_2T_3		C_2T_1		C_2T_2		C_2T_3	
	Final wt	Wt. gai. in (%)	Final wt	Wt. gai. in (%)	Final wt	Wt. gai. in (%)	Vol. change	Vol. gai. in (%)	Vol. change	Vol. gai. in (%)	Vol. change	Vol. gai. in (%)
0	2.3746	0	2.7216	0	2.2506	0	0	0.00	0	0.00	0	0.00
24	2.3776	0.02	2.7227	0.04	2.2529	0.10	58.13	2.18	3.43	0.10	17.28	0.73
48	2.3779	0.14	2.7403	0.68	2.2564	0.26	89.85	3.32	44.63	1.35	33.93	1.42
72	2.3800	0.16	2.7517	1.09	2.2669	0.72	103.3	3.81	52.51	1.59	100.0	4.07
96	2.3847	0.24	2.7541	1.18	2.2805	1.31	107.7	3.96	55.64	1.68	152.4	6.07
120	2.3895	0.44	2.7558	1.24	2.2862	1.56	120.4	4.41	68.38	2.06	166.3	6.58
144	2.3903	0.64	2.7582	1.33	2.2913	1.78	131.2	4.79	202.2	5.85	183.9	7.23
168	2.3913	0.67	2.7614	1.44	2.3079	2.48	151.9	5.50	221.6	6.38	207.4	8.08
192	2.3917	0.72	2.7615	1.44	2.3169	2.86	163.6	5.90	247.5	7.07	222.6	8.63
216	2.3917	0.73	2.7615	1.44	2.3170	2.86	173.7	6.24	259.2	7.38	246.6	9.46
240	2.3918	0.73	2.7615	1.44	2.3170	2.86	179.0	6.42	261.5	7.45	258.3	9.87

Table 17 Variation of weight gain and change in volume on 25% of fiber content for LD-PE

Time of immers in (h)	Weight of the specimen in (g)						Volume of the specimen in (mm^3)					
	C_3T_1		C_3T_2		C_3T_3		C_3T_1		C_3T_2		C_3T_3	
	Final wt	Wt. gai. in (%)	Final wt	Wt. gai. in (%)	Final wt	Wt. gai. in (%)	Vol. change	Vol. gai. in (%)	Vol. change	Vol. gai. in (%)	Vol. change	Vol. gai. in (%)
0	2.6247	0	2.4016	0	2.4219	0	0	0.00	0	0.00	0	0.00
24	2.6267	0.08	2.4018	0.01	2.4227	0.02	13.55	0.52	20.88	0.82	29.24	1.07
48	2.6356	0.41	2.4041	0.10	2.4259	0.14	22.33	0.85	27.00	1.06	41.14	1.49
72	2.6371	0.47	2.4066	0.21	2.4277	0.16	42.68	1.61	36.78	1.43	51.86	1.87
96	2.6384	0.52	2.4082	0.27	2.4290	0.24	46.27	1.74	40.10	1.56	65.64	2.36
120	2.6408	0.61	2.4112	0.39	2.4316	0.44	67.24	2.51	52.44	2.03	68.60	2.47
144	2.6647	1.50	2.4153	0.57	2.4338	0.64	91.89	3.39	75.47	2.89	104.4	3.71
168	2.6665	1.57	2.4185	0.69	2.4342	0.67	105.4	3.87	83.61	3.19	110.4	3.91
192	2.6668	1.58	2.4189	0.72	2.4343	0.72	118.2	4.32	123.7	4.66	124.1	4.37
216	2.6669	1.58	2.4189	0.72	2.4343	0.73	167.9	6.0	137.0	5.13	137.7	4.83
240	2.6669	1.58	2.4189	0.72	2.4343	0.73	178.9	6.4	138.8	5.19	139.7	4.89

Table 18 Variation of weight gain and change in volume on 15% of fiber content for LLD-PE

Time of immers in (h)	Weight of the specimen in (g)						Volume of the specimen in (mm^3)					
	C_1T_1		C_1T_2		C_1T_3		C_1T_1		C_1T_2		C_1T_3	
	Final wt	Wt. gai. in (%)	Final wt	Wt. gai. in (%)	Final wt	Wt. gai. in (%)	Vol. change	Vol. gai. in (%)	Vol. change	Vol. gai. in (%)	Vol. change	Vol. gai. in (%)
0	2.1658	0	2.1696	0	2.2154	0	0	0.00	0	0.00	0	0.00
24	2.1664	0.03	2.2388	3.09	2.2162	0.04	64.90	2.34	7.32	0.23	7.06	0.29
48	2.1673	0.07	2.2640	4.17	2.2182	0.13	78.25	2.80	306.9	8.98	77.28	3.09
72	2.1712	0.25	2.3087	6.03	2.2185	0.14	92.53	3.29	457.5	12.83	108.2	4.27
96	2.1760	0.47	2.3387	7.23	2.2194	0.18	102.4	3.64	669.1	17.71	120.9	4.76
120	2.1874	0.98	2.3722	8.54	2.2241	0.39	114.2	4.04	684.8	18.06	155.7	6.05
144	2.2034	1.70	2.4628	11.91	2.2271	0.52	149.6	5.23	691.5	18.20	186.3	7.15
168	2.2054	1.80	2.5066	13.44	2.2299	0.65	161.4	5.62	706.1	18.51	259.8	9.70
192	2.2220	2.60	2.5922	16.30	2.2223	0.76	218.4	7.45	777.5	20.01	292.0	10.78
216	2.2223	2.60	2.5923	16.31	2.2327	0.77	230.9	7.85	796.2	20.39	298.8	10.99
240	2.2223	2.60	2.5924	16.31	2.2329	0.78	242.5	8.21	798.5	20.45	301.7	11.09

Table 19 Variation of weight gain and change in volume on 20% of fiber content for LLD-PE

Immersion time in (h)	Weight of the specimen in (g)						Volume of the specimen in (mm^3)					
	C_2T_1		C_2T_2		C_2T_3		C_2T_1		C_2T_2		C_2T_3	
	Final wt	Wt. gai. in (%)	Final wt	Wt. gai. in (%)	Final wt	Wt. gai. in (%)	Vol. change	Vol. gai. in (%)	Vol. change	Vol. gai. in (%)	Vol. change	Vol. gai. in (%)
0	2.3057	0	2.7794	0	2.3078	0	0	0.00	0	0.00	0	0.00
24	2.3061	0.02	2.7896	0.37	2.3107	0.13	21.96	0.85	10.41	0.35	29.50	1.05
48	2.3121	0.28	2.7910	0.42	2.3144	0.29	48.64	1.86	86.48	2.85	57.24	2.02
72	2.3160	0.44	2.7940	0.52	2.3196	0.51	50.44	1.93	99.92	3.28	128.5	4.42
96	2.3181	0.53	2.8232	1.55	2.3269	0.82	146.7	5.42	144.2	4.67	224.3	7.47
120	2.3272	0.92	2.9645	6.24	2.3329	1.08	207.3	7.49	157.1	5.07	236.8	7.86
144	2.3283	0.97	2.9890	7.01	2.3372	1.26	219.5	7.89	159.1	5.18	248.2	8.21
168	2.3381	1.39	2.9990	7.32	2.3382	1.30	248.1	8.83	175.6	5.63	269.1	8.84
192	2.3468	1.75	2.9996	7.34	2.3545	1.98	247.3	8.77	211.6	6.71	286.7	9.33
216	2.4369	1.75	2.9998	7.35	2.3552	2.01	281.9	9.92	225.7	7.12	306.6	9.95
240	2.3470	1.76	2.9998	7.35	2.3552	2.01	297.0	10.5	235.9	7.42	318.4	10.29

Table 20 Variation of weight gain and change in volume on 25% of fiber content for LLD-PE

Time of Immers in (h)	Weight of the specimen in (g)						Volume of the specimen in (mm^3)					
	C_3T_1		C_3T_2		C_3T_3		C_3T_1		C_3T_2		C_3T_3	
	Final wt. (g)	Wt. gai. in (%)	Final wt. (g)	Wt.gai.in (%)	Final wt. (g)	Wt. gai. in (%)	Vol. change	Vol. gai in (%)	Vol. change	Vol. gai in (%)	Vol. change	Vol.gai in (%)
0	2.4206	0	2.2025	0	1.5706	0	0	0.00	0	0.00	0	0.00
24	2.4401	0.79	2.2039	0.06	1.5783	0.49	22.65	0.75	12.12	0.47	10.22	0.42
48	2.5380	4.64	2.2492	0.29	1.6031	2.03	75.03	2.43	22.83	0.89	37.35	1.52
72	2.6291	7.93	2.2590	2.50	1.6322	3.77	124.7	3.97	35.54	1.37	40.31	1.64
96	2.6404	8.32	2.2613	2.60	1.6529	4.98	158.9	5.01	113.6	4.26	88.97	3.55
120	2.7388	11.62	2.2731	3.11	1.6805	6.54	186.0	5.81	116.8	4.37	101.8	4.04
144	2.7392	11.63	2.2769	3.27	1.6888	6.99	195.1	6.08	119.1	4.45	106.7	4.23
168	2.7398	11.63	2.2777	3.30	1.6937	7.27	218.5	6.76	133.1	4.95	118.9	4.69
192	2.8026	13.63	2.2794	3.37	1.7260	9.01	221.8	6.85	138.0	5.11	140.2	5.49
216	2.8026	13.63	2.2795	3.38	1.8198	13.7	222.7	6.87	158.7	5.85	150.9	5.88
240	2.8026	13.63	2.2795	3.38	1.8198	13.7	222.8	6.87	170.7	2.26	155.3	6.04

temperature and the result showed that maximum water absorption was exhibited by C_2T_3 for LD-PE and C_3T_3 for LLD-PE composite materials, while 25/65% weight ratio of hybrid composites had minimum moisture absorption content compared to other weight ratios of fiber composites in both materials. Similarly, a 25/65% weight ratio of LLD-PE composites materials was gained a maximum change volume ratio than the LD-PE composites. Moisture absorption by immersion method was evaluated at different injection temperatures and fiber composition as shown in Figs. 15, 16, 17, 18, 19 and 20 for LD-PE and LLD-PE composite materials. The hybrid composites showed a Fickian diffusion behavior, but with a deviation at high temperatures, which was attributed to the formation of microcracks and dissolution of lower molecular weight substances from the natural fibers.

3.4.1 Measurement of diffusivity

The water absorption of ensete and sisal hybrid reinforced polyethylene composite has been studied through the diffusion constants *k* and *n*. The behaviour of moisture absorption in the composite was studied by the shape of the curve represented by the Eq. (8) [21]:

$$M_t/M_n = kt^n \tag{8}$$

where M_t is the moisture content at a specific time'*t*', M_n is the equilibrium moisture content (EMC), and *k* and *n* are constants.

The value of *k* and *n* were found out from the slope and the intercept of M_t/M_m versus time '*t*' in the log plot which was drawn from the data obtained from the experiment of moisture absorption with time. Figures 21, 22, 23, 24, 25 and 26 showed the typical curve of log (M_t/M_m) as a function of log (*t*) for both LD-PE and LLD-PE composites respectively, used to determine these constants. The values of *k* and *n* resulting from the fitting of all formulations are shown in Table 21. It was observed that the value of *n* is close to 0.3 for all of the composites. This confirms that Fickian diffusion can be used to adequately describe moisture absorption in the composites. A higher value of *n* and *k* indicates that the composite needs a shorter time to attain equilibrium water absorption. The value of *n* and *k* was found to increases with increasing fibre content for LLD-PE composite materials but, decreases in increasing injection temperature resulting in higher moisture absorption initially. The value of *k* and *n* in LLD-PE composites were relatively higher than that of LD-PE composite materials. The diffusion coefficient or diffusivity (*Dx*) of moisture absorption was calculated using the following equation:

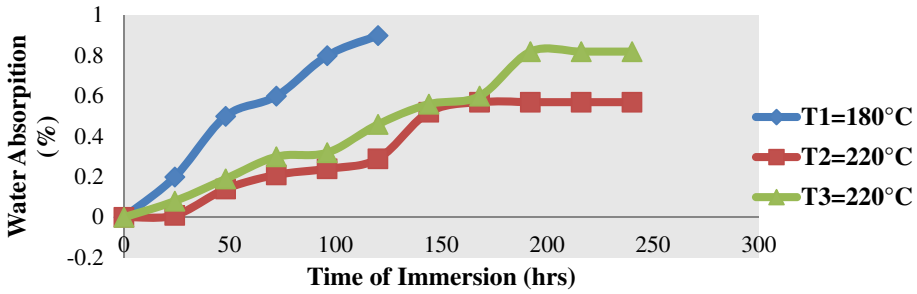

Fig. 15 Variation of water absorption for 15% of fiber composition for LD-PE composite materials with immersion time at different injection temperature

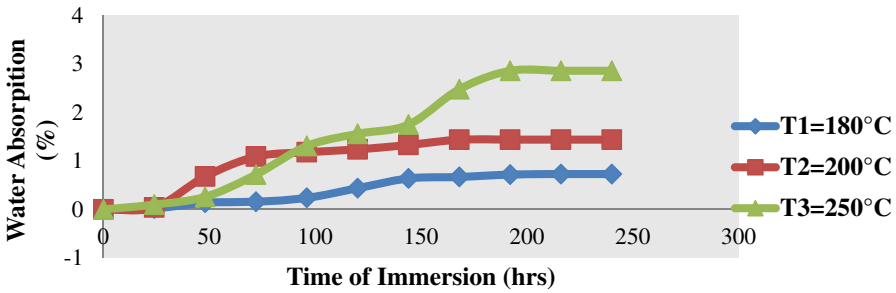

Fig. 16 Variation of water absorption for 20% of fiber composition for LD-PE composite materials with immersion time at different injection temperature

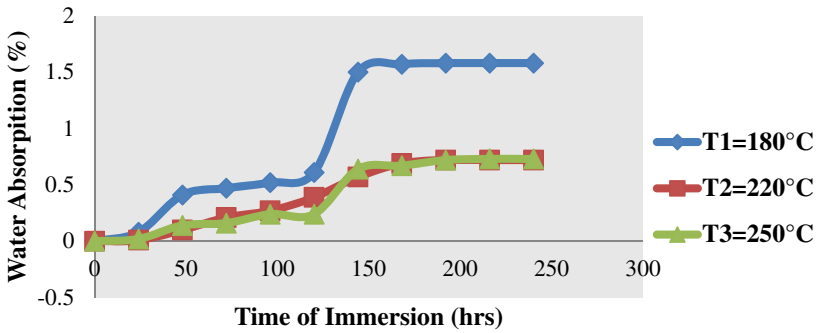

Fig. 17 Variation of water absorption for 25% of fiber composition for LD-PE composite materials with immersion time at different injection temperature

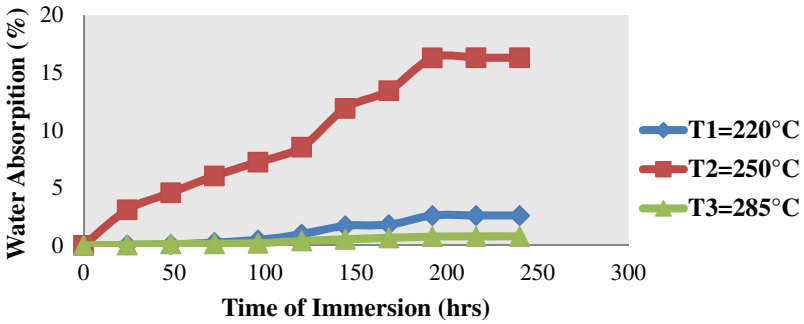

Fig. 18 Variation of water absorption for 15% of fiber composition for LLD-PE composite materials with immersion time at different injection temperature

$$D_x = \pi \left[\frac{h}{4M_m}\right]^2 \left[\frac{M_2 - M_1}{\sqrt{t_2} - \sqrt{t_1}}\right]^2 \quad (9)$$

where 'M_m' is the maximum percentage of moisture content, 'h' is the sample thickness, 't_1' and 't_2' are the selected points in the initial linear portion of the graph of moisture absorption (M_t) versus square root of time (t) as shown in Figs. 27, 28, 29, 30, 31 and 32 for LD-PE and LLD-PE composite materials and 'M_1' and 'M_2' are the respective moisture content.

From the plot of M_t versus square root of time (t), the value of D_x has been evaluated and summarized in

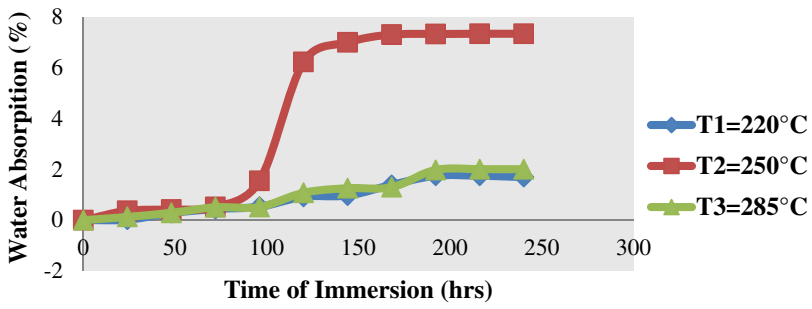

Fig. 19 Variation of water absorption for 20% of fiber composition for LLD-PE composite materials with immersion time at different injection temperature

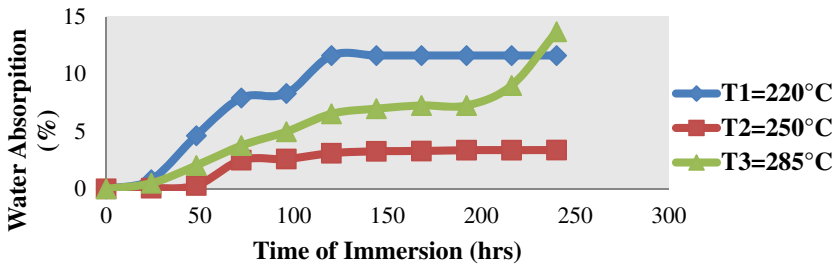

Fig. 20 Variation of water absorption for 25% of fiber composition for LLD-PE composites materials with immersion time at different injection temperature

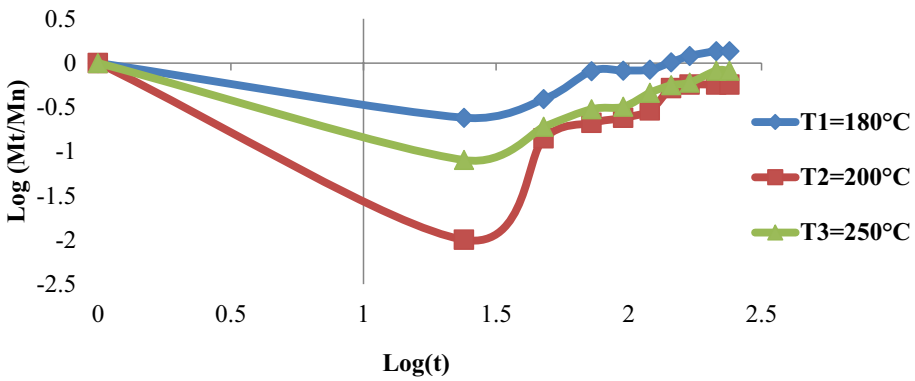

Fig. 21 Variation of log (M_t/M_m) with log (t) for 15% of fiber composition for LD-PE composites materials with immersion time at different injection temperature

Table 22 for both LD-PE and LLD-PE composite materials. In the case of LD-PE, It has been observed D_x value is high for C1 fiber composition at temperature T_1=180 °C while in the case of LLD-PE composite materials the value of D_x is high for C_2 fiber composition at T_2=250 °C.

The comparison of different composite materials and polyethylene plastic materials as shown in Table 23.

3.5 Microstructure of the hybrid composites

The optical microscopy (OM) micrographs are used to observe the internal cracks, fractured surfaces and internal structure of the tested samples of the ensete/sisal fiber-reinforced composites. The microstructure view of composite materials is as shown in Figs. 33 and 34. It represents the appearance of the polished samples as a basis for an estimate of the reinforcement distribution in the matrix substrate. A microstructural characterization was also performed to evaluate the influence of the fiber content on the processing temperature, in the microstructure specimens of different composite materials at the same fiber composition and, on the other hand, the incorporation of reinforcement/filler materials with that of the polymer. These show that the smaller percent of reinforced particles are prone to forming the clusters, while the distribution of the highest percent particle is favorable interims of mechanical properties, which means that as shown from the microstructural result a composite having higher percentage of fiber composition has more compatible than the smaller one.

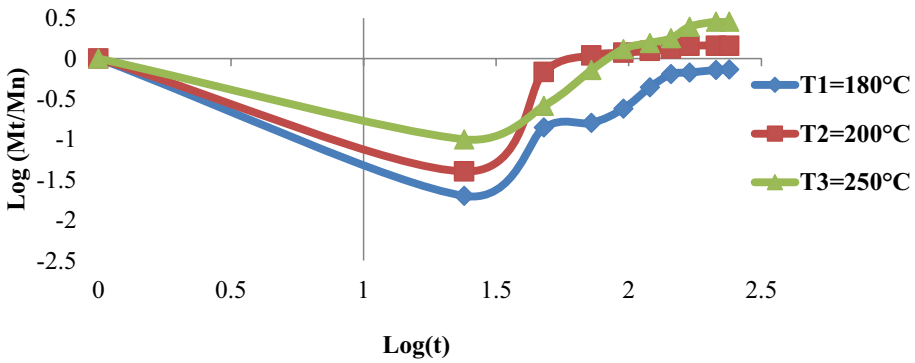

Fig. 22 Variation of log (M_t/M_m) with log (t) for 20% of fiber composition for LD-PE composites materials at different injection temperature

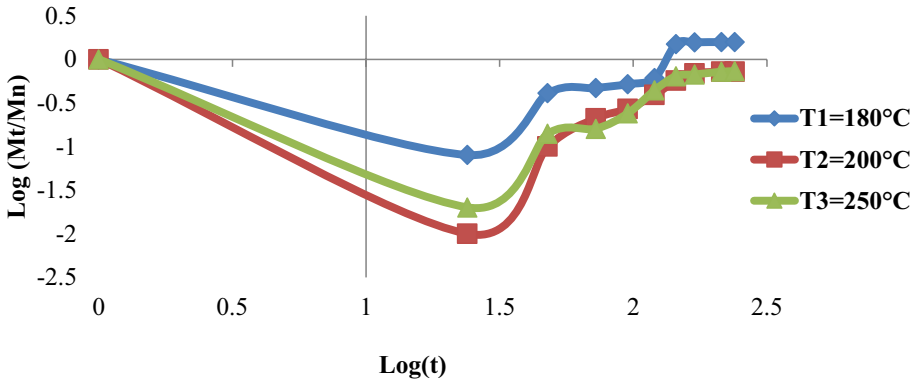

Fig. 23 Variation of log (M_t/M_m) with log (t) for 25% of fiber composition for LD-PE composites materials at different injection temperature

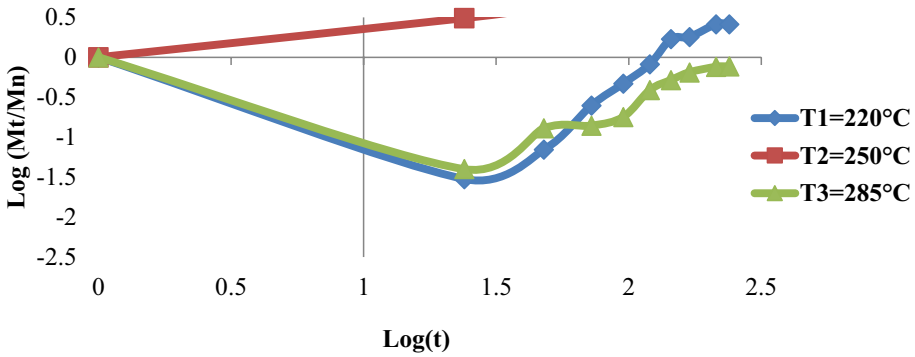

Fig. 24 Variation of log (M_t/M_m) with log (t) for 15% of fiber composition for LLD-PE composite materials at different injection temperature

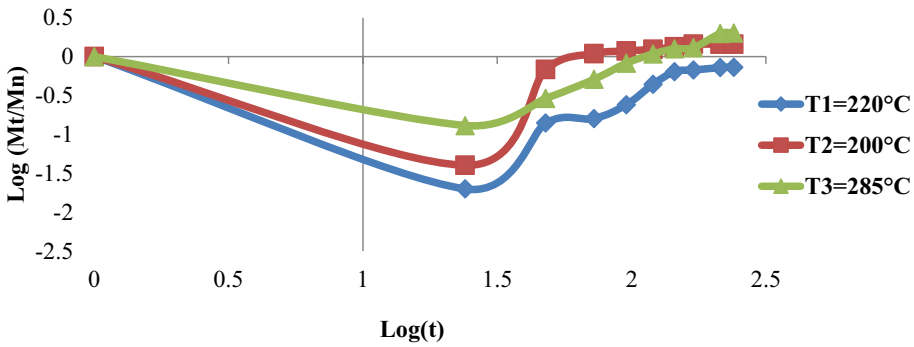

Fig. 25 Variation of log (M_t/M_m) with log (t) for 20% of fiber composition for LLD-PE composite materials at different injection temperature

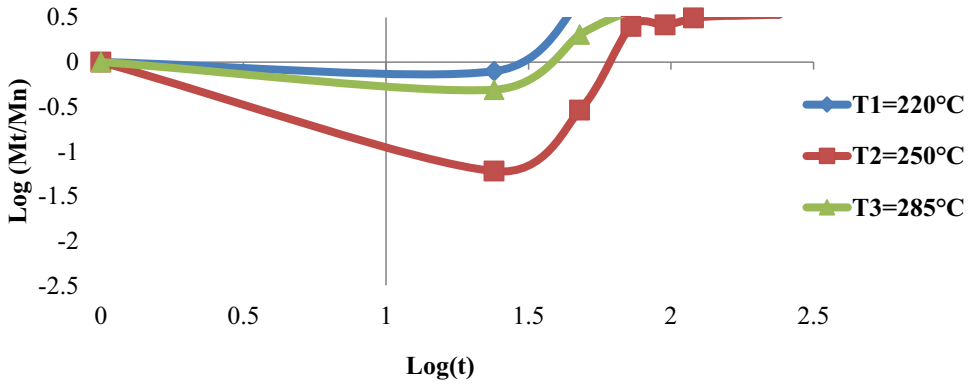

Fig. 26 Variation of log (M_t/M_m) with log (t) for 25% of fiber composition for LLD-PE composite materials at different injection temperature

Table 21 Diffusion case selection parameters

Composite materials	Composition (%)	Inj. temrature (°C)	n	k	Composite materials	Composition (%)	Inj. temrature (°C)	n	k
LD-PE	C_1	$T_1 = 180$	0.1272	0.0032	LLD-PE	C_1	$T_1 = 220$	0.3589	0.0054
		$T_2 = 200$	0.2598	0.0014			$T_2 = 250$	0.2724	0.0373
		$T_3 = 250$	0.1604	0.0023			$T_3 = 285$	0.1949	0.0017
	C_2	$T_1 = 180$	0.2354	0.0016		C_2	$T_1 = 220$	0.3394	0.0039
		$T_2 = 200$	0.2699	0.0038			$T_2 = 250$	0.3249	0.0209
		$T_3 = 250$	0.2782	0.0063			$T_3 = 285$	0.2159	0.0045
	C_3	$T_1 = 180$	0.2032	0.0029		C_3	$T_1 = 220$	0.3609	0.0363
		$T_2 = 200$	0.2816	0.0016			$T_2 = 250$	0.3442	0.0073
		$T_3 = 250$	0.2091	0.0012			$T_3 = 285$	0.3738	0.0237

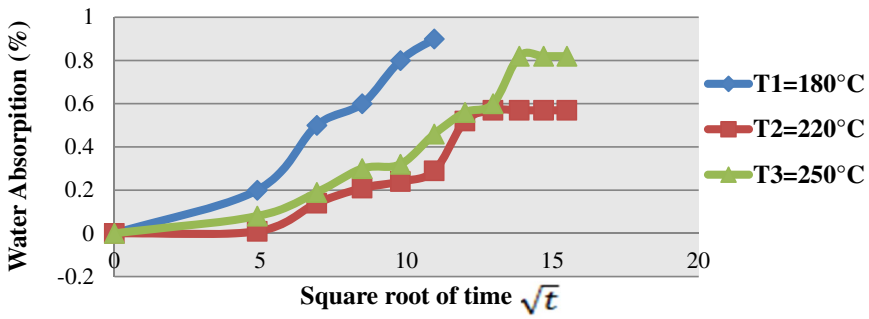

Fig. 27 The percentage of moisture absorption versus square root of time for calculation of diffusivity for 15% of the fiber of LD-PE materials

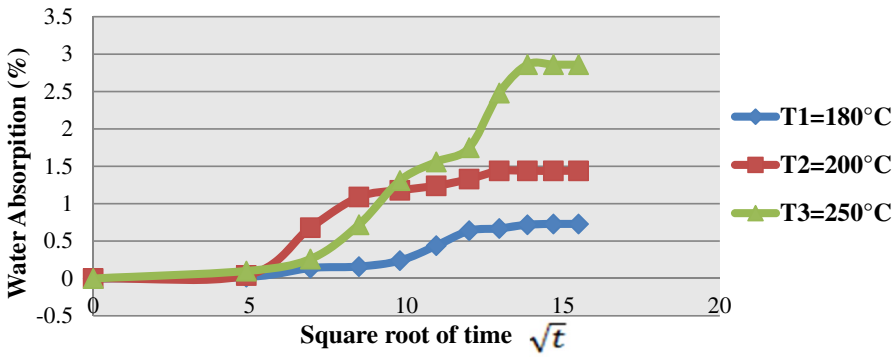

Fig. 28 The percentage of moisture absorption versus square root of time for calculation of diffusivity for 20% of the fiber of LD-PE materials

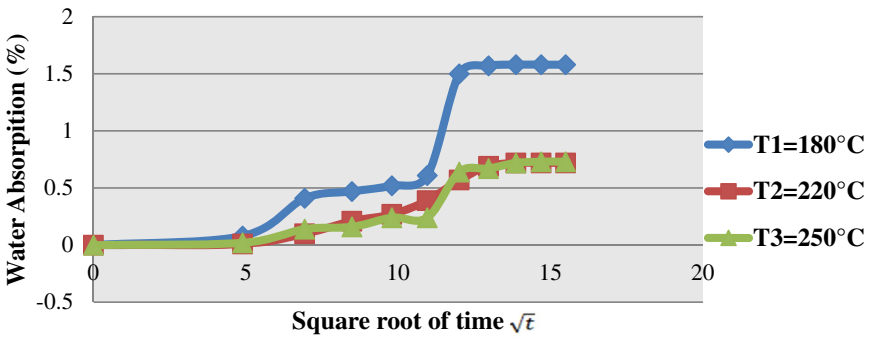

Fig. 29 The percentage of moisture absorption versus square root of time for calculation of diffusivity for 25% of the fiber of LD-PE materials

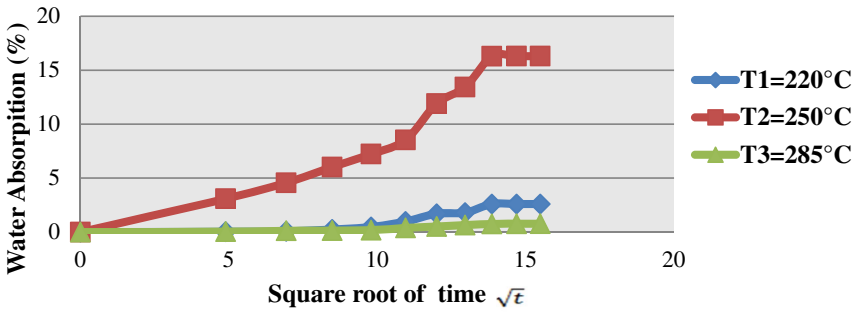

Fig. 30 The percentage of moisture absorption versus square root of time for calculation of diffusivity for 15% of the fiber of LLD-PE materials

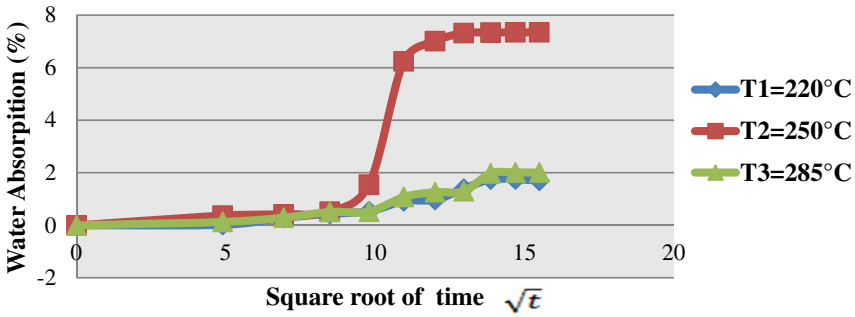

Fig. 31 The percentage of moisture absorption versus square root of time for calculation of diffusivity for 20% of the fiber of LLD-PE materials

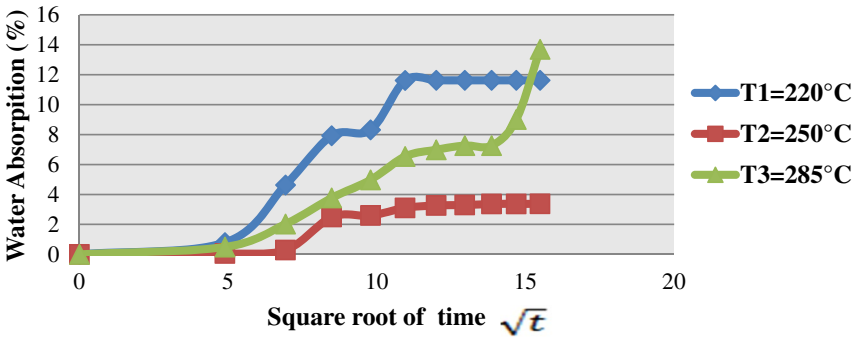

Fig. 32 The percentage of moisture absorption versus square root of time for calculation of diffusivity for 25% of the fiber of LLD-PE materials

Table 22 Diffusivity for hybrid of ensete and sisal reinforced fiber polyethylene composites at different injection temperature

Composite materials	Composition (%)	Inj. temprature (°C)	Diffusivity (D_x) × 10^{-4}	Composite materials	Composition (%)	Inj. temprature (°C)	Diffusivity (D_x) × 10^{-4}
LD-PE	C_1	$T_1 = 180$	4.724412	LLD-PE	C_1	$T_1 = 220$	0.564406
		$T_2 = 200$	0.915316			$T_2 = 250$	4.301038
		$T_3 = 250$	0.228775			$T_3 = 285$	1.097752
	C_2	$T_1 = 180$	0.405728		C_2	$T_1 = 220$	1.076484
		$T_2 = 200$	0.755592			$T_2 = 250$	8.788526
		$T_3 = 250$	0.931092			$T_3 = 285$	1.044118
	C_3	$T_1 = 180$	0.140814		C_3	$T_1 = 220$	0.687289
		$T_2 = 200$	0.275750			$T_2 = 250$	0.047002
		$T_3 = 250$	0.122340			$T_3 = 285$	0.214034

Table 23 The comparison result of composite material and Polyethylene plastic materials

Test name	Hybrid composite materials		Plastic materials	
	ESHF-LD-PE	ESHF-LLD-PE	LD-PE	LLD-PE
Tensile strength (N/mm^2)	41 (C_1T_2)	66 (C_3T_2)	38 (T_2)	31 (T_2)
Flexural strength (N/mm^2)	7.96 (C_1T_2)	11.94 (C_3T_2)	3.98 (T_2)	5.97 (T_2)
Compression strength (N/mm^2)	56.51 (C_1T_2)	14.42 (C_1T_3)	10.31 (T_2)	10.67 (T_2)
Water absorption test (wt%)	0.72 (C_1T_2)	0.78 (C_1T_3)	14.65 (C_1T_2)	16.8 (C_1T_2)

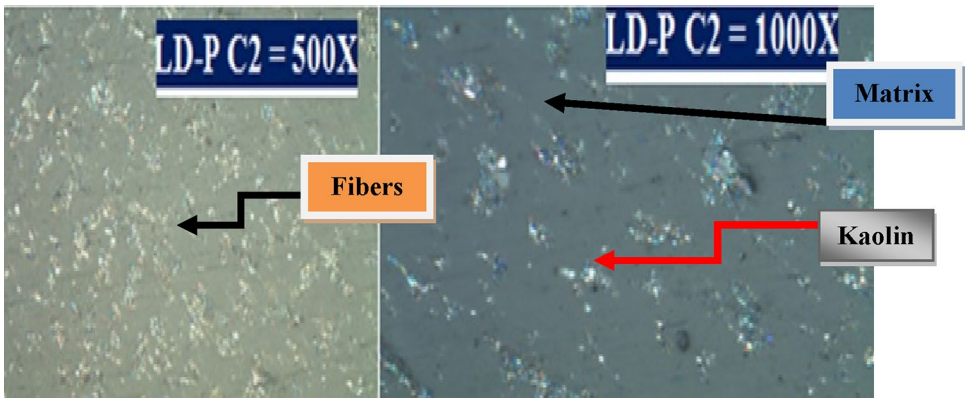

Fig. 33 Microstructures views of LD-PE for 20% of fiber composition

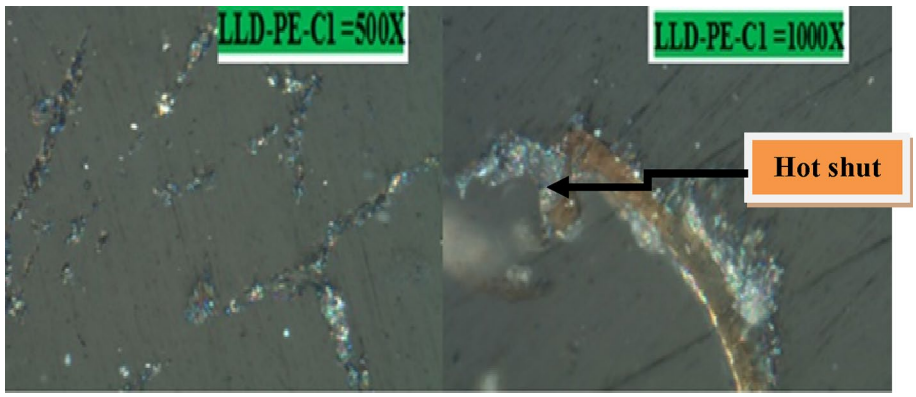

Fig. 34 Microstructures views of LLD-PE for 25% of fiber composition

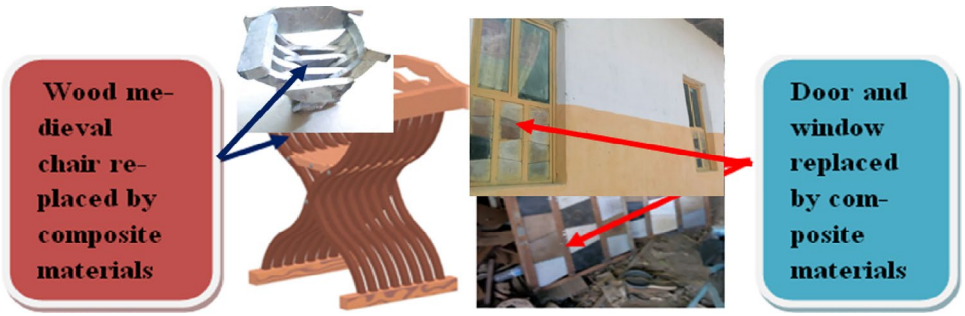

Fig. 35 Composite product materials for different applications

4 Conclusion and recommendation

4.1 Conclusion

The hybrid composites which contains 15% sisal and ensete fiber with 65% LLD-PE matrixes (Composition, C_3 at T_2) have more tensile, flexural and compression strength than other composites can withstand the tensile strength of 66 MPa and flexural strength of 11.94 MPa and compression strength of 56.5 MPa followed by 20 % sisal and ensete fiber with 70% of the same matrices (composition C_2 of T_1 and $T_{2)}$ which holds 65 MPa and 9.95 MPa respectively, Which is 56.58%, 163.90%, and 69.43% higher than that of the non-reinforced PE respectively. The microstructural properties of LD-PE/LLD-PE ESHF composite samples were characterized by micrographs of the specimen by OPM illustrated good bonding and compatibility between the fibers and matrix. As ensete fiber is known for its remarkable smoothness its mixture with sisal fiber will lead towards better surface finish of the product with desired strength. This study, therefore, indicated that sisal and ensete fiber are a successful solution for many load-bearing and structural applications such as construction, furniture making and automotive. Fillers have been used in this composite. Although the filler is typically added to improve the fire resistance, reduce the cost of a composite

and also reduce the voids and improve the processing viscosity. Water absorption is one of the major concerns in using natural fiber composites in many applications. In this study, 24, 48, 96, 120, 144, 168, 216 and 240-h water absorption was measured by the weight change method for the ensete/sisal hybrid fibers reinforced in polyethylene composites materials. The water absorption in hybrid composites was negligible. Because in 24 h, maximum and minimum water uptake was 0.1 and 0.6% respectively. To conclude, the highest rate of water uptake of natural fiber composites was 16.31%, which was obtained at 225 °C processing temperature and 25% fiber loading in 240 h. The hydrophilic nature of natural fibers is incompatible with the hydrophobic polymer matrix and tends to form aggregates. These hydrophilic fibers exhibit poor resistance to moisture, which leads to high water absorption, subsequently resulting in poor tensile properties of the natural fiber-reinforced composites. In the beginning, it absorbs water at an increased rate before it attains the maximum, the rate drops drastically until reaches a saturation point. The 20 wt% of the fiber for all samples attains saturation earlier than the other test specimen. When weight gain is more, water molecules interlocked in the composites are more. Thus, the water molecules get chances to attack the interface adhesion resulting in bonding of the fiber and the matrix internally in the composite. Thus, it evidenced clearly that the immersion time influences the absorption behavior of the sisal and ensete fiber reinforced polyethylene composites variedly. From the above citations and discussions, it can be found that the values of the tensile strength of natural fibre reinforced composites increased with increasing fibre loading up to a maximum or optimum value before falling back. However, it is generally true that the values of Young's modulus increased progressively with increasing fibre loading. On the other hand, some researchers found the opposite trend to the increase of composite strength with increasing fibre content. This can be attributed to many factors such as incompatibility between matrix and fibers, improper manufacturing processes, fiber degradation, and others.

4.2 Recommendation

The composite terminal box closure material is recommended for composite quality application at best injection temperature of not greater than 285 °C because at a higher temperature, fibre degradation might have occurred, therefore, this leads to inferior tensile properties. However, the injection temperature should not be lower than 175 °C to ensure adequate melting of the matrix in comparison with other studies of the same fiber composition. The injection temperature of the composite was improved by 42.5% (200–285 °C) of the processing temperature. This study, therefore, suggested that these hybrid composites can be used as in an automobile, construction and household applications like the manufacturing of tables, chairs, door panels, interior paneling, door-frame profiles, food trays, partitions, bath units, lampshades, suitcases, helmets, etc. as shown in Fig. 35.

Acknowledgements We would like to thank the manager of the Metal Industry Development Institute, Addis Ababa for providing us an opportunity to use their machines and respecting departmental facilities.Finally, we would like to thanks the Department of Mechanical Design and Manufacturing Engineering, Adama Science and Technology University.

Compliance with ethical standards

Conflict of interest The authors declare that they have no conflict of interest.

References

1. Nazmul PMD (2016) The prospects and challenges of plastic industries Bangladesh. Plastic Technology, Arcada, pp 12–15
2. Sathishkumar TP, Naveen J, Satheeshkumar S (2014) Hybrid fiber reinforced polymer composites—a review. J Reinf Plast Compos 33(5):454–471
3. KoniuszewskaAG, Kaczmar JW (2017) Application of polymer based composite materials in transportation
4. Malikane C, Roberts S, Sikhweni N (2000) Competition and market structure in the plastics sector
5. Rohan T, Tushar B, Mahesha GT (2018) Review of natural fiber composites. Int Conf Adv Metall Mater Manuf. https://doi.org/10.1088/1757-899X/314/1/012020.pp1-10
6. Muller M, Valasek P, Ruggiero A (2017) Strength characteristics short-fiber composites from the plant ensete ventricosum. Short-Fibre Compos BioResour Com 12(1):255–269
7. Mehamud I, Raj J, Zeleke C, Gebre T (2016) Fabrication and mechanical property evaluation of ethiopia banana fiber reinforced polymer composites. Adv Res 7(5):1–10
8. Adhikari M (2012) Natural fibre composites for injection molding. Plastic Technology, Arcadia, pp 16–20
9. Thiruvasagam C, Harish R, Tamilarasan S, Venkatesh G, Vimalathithan K (2016) Evaluation of mechanical properties of banana fiber–jute–glass fiber reinforced polyester composite. Int J Innov Res Sci Eng Technol (IJIRTSE) 2(7):29–37
10. Adeosun SO, Usman MA, Akpan EI, Dibie WI (2014) Characterization of LDPE reinforced with calcium carbonate-fly ash hybrid filler. J Min Mater Charac Eng 2:334–345
11. Sanjeevamurthy GC, Srinivas G Effect of alkali treatment, fiber loading and hybridization on tensile properties of sisal fiber, banana empty fruit bunch fiber and bamboo fiber reinforced thermo set composites.
12. Mizera C, Herak D, Hrabe P, Kabutey A (2017) Effect of temperature and moisture content on tensile behavior of false banana fibre (*Ensete ventricosum*). Int Agrophys 33:377–382
13. de Andrade F, Silva NC, Filho RDT (2010) Mechanical behavior of natural sisal fibers. J Biobased Mater Bioenergy 4:1–8
14. Alhayat, Temesgen G, Sahu O (2014) Process ability enhancement of false banana fibre for rural development. J Agric Econ Exten Rural Dev 1(6):064–073

15. Wang J, Chen D, Wang S, Ziran Du, Jiang N, Peng J (2017) Insert injection molding of low-density polyethylene single-polymer composites reinforced with ultrahigh molecular-Weight polyethylene fabric. J Thermoplast Compos Mater. https://doi.org/10.1177/0892705717734593
16. Lal SK, Vasudevan H (2013) Optimization of injection moulding process parameters in the moulding of low-density polyethylene (LDPE). Int J Eng Res Dev 7(5):35–39
17. Kale HP, Hambire UV (2015) Review on optimization of injection molding process parameter for reducing shrinkage of high-density polyethylene (HDPE) material. Int J Sci Res 4(4):2847–2850
18. Muhd Hasanul Isyraf Mat Junoh (2015) Injection molding parameters optimization for polymer matrix composite polypropylene reinforced wood fiber. J Basic Appl Sci Res 5(8):49–53
19. Dan-asabe B, Yaro SA, Yawas DS, Aku SY (2017) Statistical modeling and optimization of the flexural strength, water absorption and density of a doum palm-kankara clay filler hybrid composite. J King Saud Univ Eng Sci (in press)
20. Marom G (1985) The role of water transport in composite materials; chapter-9. In: Comyn J (ed) Polymer permeability. Elsevier Applied Science, Amsterdam
21. Chiou JS, Paul DR (1986) Sorption equilibria and kinetics of ethanol in miscible poly(vinylidene fluoride)/poly(methyl methacrylate) blends. J Polym Eng Sci 26:1218–1227